Available online at www.sciencedirect.com
SCIENCE DIRECT®
Surface and Coatings Technology 177–178 (2004) 459–468
SURFACE & COATINGS TECHNOLOGY
www.elsevier.com/locate/surfcoat

# Microstructure, mechanical properties and cutting performance of superhard (Ti,Si,Al)N nanocomposite films grown by d.c. reactive magnetron sputtering

S. Carvalho[a,*], E. Ribeiro[a], L. Rebouta[a], C. Tavares[a], J.P. Mendonça[b], A. Caetano Monteiro[b], N.J.M. Carvalho[c], J.Th.M. De Hosson[c], A. Cavaleiro[d,e]

[a]*Dept. Física (GRF), Universidade do Minho, Campus de Azurém, 4800-058 Guimaraes, Portugal*
[b]*Dept. Mecânica, Universidade do Minho, Campus de Azurém, 4800-058 Guimaraes, Portugal*
[c]*Department of Applied Physics, University of Groningen, 9747 AG Groningen, The Netherlands*
[d]*Laboratoire de Metallurgie Physique, Université de Poitiers, 86960 Futuroscope, France*
[e]*ICEMS—Fac. de Ciências e Tecnologia da Universidade de Coimbra, 3030 Coimbra, Portugal*

**Abstract**

This paper reports on the optimization of coating properties to improve the performance of tools in severe cutting conditions. Tungsten carbide tools coated with (Ti,Si,Al)N films deposited by d.c. reactive magnetron sputtering have been investigated. The structure and the hardness of the coated samples were analyzed by X-ray diffraction (XRD) and depth-sensing indentation, respectively. XRD results revealed a structure indexed to fcc TiN. The tool life and tool failure modes were examined for various cutting conditions. A promising wear performance of the (Ti,Si,Al)N coatings was confirmed by scanning electron microscopy observations complemented with energy dispersive X-ray spectrometry analysis. At higher cutting speed (200 m/min) it seems that after turning 15 min the cutting performance of (Ti,Si,Al)N coated tools is better than that presented by the commercial multilayer coating ($TiCN/Al_2O_3/TiN$)—which was used as a reference. Also regarding the final surface finish of the steel workpiece, the (Ti,Si,Al)N coatings outperformed the commercial tool, considering that the roughness of the workpiece is smaller in the former case (4 μm) than that measured in the latter one (12 μm).


*Keywords:* (Ti,Si,Al)N; Multilayers; XRD; Cutting tools; Wear

## 1. Introduction

Increasing requirements on high speed and dry cutting applications open up new demands on the quality of cutting tool materials. Traditional hard coatings, as TiN single layer coatings, played an important role in the development stage to improve the wear resistance of cutting and forming tools. One of the drawbacks of TiN is its limited oxidation resistance to the high temperatures that can be reached during the cutting process. The temperature at the contact between the chip and the tool can rise up to 1200 °C [1,2]. For these extreme cutting conditions (high temperatures/oxidation) chemical resistance is one of the most important requirement for a hard coating [3]. Cubic boron, c-BN, nitride coatings were being considered the best solution for cutting applications, such as steel machining, due to their chemical resistance and hardness at the high cutting temperatures [4]. Nevertheless, c-BN deposited by PACVD suffers from too high compressive internal stresses that can lead to the premature failure of the tools [5]. (Ti,Al)N coatings can also be an alternative since they exhibit a great improvement in the oxidation resistance when compared to TiN coatings, being possible to use them at temperatures up to 800 °C [6,7]. Thus, the most important criteria for the selection of a coating material for tribological applications include resistance against oxidation, high hardness, high stiffness and a low coefficient of friction. Recently, nanocomposite coatings have attracted increasing interest due to the possibility to combine all of these properties. Among them, coatings of the (Ti,Si)N system were the most studied [8–11], having been suggested that their nanostructure consisted of cubic TiN nanocrystallites embed-

*Corresponding author. Tel./fax: +351-253-510470.
*E-mail address:* nocas@fisica.uminho.pt (S. Carvalho).

0257-8972/04/$ - see front matter © 2003 Elsevier B.V. All rights reserved.
doi:10.1016/j.surfcoat.2003.08.056

ded in an amorphous matrix of silicon nitride. The superhardness of these composites was attributed to the strong resistance of both the crystalline (nc-TiN) and amorphous (a-$Si_3N_4$) phases having a high cohesive energy at the interface. The usual mechanisms of plastic deformation and crack propagation are absent or hindered allowing that the mechanical failure in such material only arises for very high loading [12]. Previous research work with (Ti,Si,Al)N system [13,14] also demonstrated that the deposited films could belong to this class of nanocomposite materials. It was shown that the hardness increases with small Si additions to the (Ti,Al)N system, the maximum values being reached for a Si content between 2 and 6.5 at.%; the values were in the range 45–57 GPa [15]. Also, an increase in the thermal stability of these coatings was observed being allowed temperatures over 900 °C without significant structural transformations [16]. Furthermore, Vaz et al. [17] have shown that $Ti_{0.27}Al_{0.53}Si_{0.2}N$ coating exhibited a better oxidation resistance at 900 °C than $Ti_{0.35}Al_{0.65}N$ coating.

Nanocomposite (Ti,Si,Al)N and (Ti,Al)N coatings have been deposited onto cermet cutting tools and were compared with a commercial coating (one of the best solutions actually available in the market for high-speed turning, consisting of a multilayer formed by TiCN, $Al_2O_3$ and TiN, deposited by thermal CVD only suitable for coating high temperature resistant substrates such as cemented carbides) used as reference, when tested in dry cutting operation. The overall aim of this work is to ascertain if coatings of the Ti–Si–Al–N quartenary system provide an alternative to TiN or (TiAl)N coatings for industrial applications. The correlation between (Ti,Al,Si)N properties and wear behaviour will be discussed in detail, as well as the wear mechanisms.

## 2. Experimental details

### *2.1. Deposition of the coatings*

(Ti,Si,Al)N coatings were deposited on cutting tools of WC–Co by reactive magnetron sputtering, in a Ar/N2 atmosphere, using a custom made equipment. Rectangular magnetron cathodes of the type 2 were used in a closed field configuration. Two series of samples were produced. In the first group of the coatings two magnetrons, vertically opposite, with a $Ti_{0.5}Al_{0.5}$ target and a Ti target with some incrusted Si pieces, were used for the coatings deposition. The current density applied to both magnetrons was approximately 10 mA/cm$^2$. Prior to the final, an adhesion layer of TiAl, with a thickness of approximately 0.25 μm, was deposited. In the second group of samples the four magnetrons were used with respectively, a $Ti_{0.5}Al_{0.5}$ target, a Ti target, another Ti target incrusted with Si pieces, being the fourth a decoy magnetron without a target. In the active cathodes, the current density was varied in the range 0–10 mA/cm$^2$. A Ti adhesion interlayer was deposited since a better result can be achieved when comparing to TiAl. The cutting tools were placed in a substrate holder with a planetary twofold rotation system, and a bias voltage of −70 V was applied during the deposition. The substrate temperature was kept approximately constant at 200 °C.

Energy dispersive X-ray spectrometry (EDS) and X-ray diffraction (XRD) were used in order to evaluate the chemical composition and the microstructure of the coatings, respectively. Hardness and Young's modulus were determined by depth sensing microindentation. Table 1 summarizes the deposition parameters and the main properties of the studied coatings.

### *2.2. Turning test*

A Cincinnati Milacron Hawk-150 numerically controlled lathe was used to perform the machining experiments. These turning tests were performed in different machining conditions (Table 2) using steel working material. The steel chosen is a usual commercial alloy steel, with main applications in chafts, bearings and some plastic moulds. Dry turning was used; though eliminating coolant increases the amount of heat at the cutting zone, creating the potential for premature tool wear, machining severe conditions were this way better simulated. The following conventional tool wear parameters were measured by scanning electron microscopy (SEM) and with a confocal microscope: VB—maximum flank wear, KT—maximum crater depth, KM—distance between tool edge and crater centre (rake face). After the turning tests, the dominant wear mechanisms were revealed by morphological and chemical modifications observed by SEM coupled with an EDS microanalyzer.

The thickness of the coatings was evaluated by SEM. The commercial cutting tool was known to be produced by CVD; the coating comprised a 8.8 μm Ti(C,N) base layer, a 4.3 μm intermediate $Al_2O_3$ layer and a 1.6 μm top TiN layer.

## 3. Results

### *3.1. Microstructure of the as-deposited coatings*

#### *3.1.1. X-ray diffraction analysis*

The diffraction peaks detected in the XRD patterns for the two sets of coatings evaluated are displayed in Fig. 1. An analysis of all the XRD diffractograms allows to detect a mixture of crystalline phases that can be indexed as a fcc structure similar to TiN. For the particular case of the (Ti,Al)N sample (without Si) a lattice parameter of 4.19 Å was obtained (tool 7). This is related with the formation of a solid solution where Al atoms substitute Ti atoms in TiN cubic lattice (remaining still a fcc structure) [18]. When the deposi-

Table 1
Some experimental parameters and properties relative to the sputtered samples

| Tool | Composition[a] | Number of magnetrons | $J_{TiSi}$ (mA/cm$^2$) | $J_{TiAl}$ (mA/cm$^2$) | Interlayer | Thickness ($\mu$m) | Hardness (GPa)[b] | Young's modulus (GPa)[b] | Residual stress (GPa)[c] |
|---|---|---|---|---|---|---|---|---|---|
| Commercial | TiN | – | – | – | $Al_2O_3$—4.3 $\mu$m[d] Ti(C,N)—8.8 $\mu$m[d] | 1.6[d] | $22 \pm 7$ | $348 \pm 84$ | 0.2 |
| P3 | $Ti_{0.82}Si_{0.08}Al_{0.14}N_{0.96}$ | 2 | 10 | 10 | TiAl—0.2 $\mu$m[d] | 3.7[d] | $35 \pm 5$ | $379 \pm 58$ | $-4.9$ |
| P7 | $Ti_{0.56}Al_{0.46}N_{0.98}$ | 4 | 0 | 10 | Ti | $\approx 3$ | $12 \pm 3$ | $369 \pm 80$ | $-4.5$ |
| P10 | $Ti_{0.86}Si_{0.03}Al_{0.16}N_{0.95}$ | 4 | 5 | 5 | Ti | $\approx 3$ | $12 \pm 2$ | $288 \pm 63$ | $-2.8$ |
| P6 | $Ti_{0.86}Si_{0.04}Al_{0.18}N_{0.92}$ | 4 | 10 | 10 | Ti | $\approx 3$ | $25 \pm 4$ | $394 \pm 68$ | $-0.6$ |

All the samples were produced with 200 °C as the substrate temperature.
[a] Measured by EDS.
[b] Measured by ultramicrohardness.
[c] Measured by $\sin^2 \psi$ method.
[d] Measured by SEM.

Table 2
Tool wear data after turning under various cutting conditions and roughness of the workpiece

| 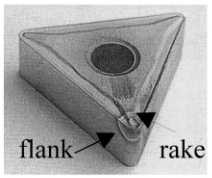  | $v=100$ m/min, $t=15$ min, $f_n=0.1$ mm/rev | | | | $v=200$ m/min, $t=15$ min, $f_n=0.1$ mm/rev | | | | | $v=200$ m/min, $f_n=0.1$ mm/rev |
|---|---|---|---|---|---|---|---|---|---|---|
| | KT (μm) | KM (μm) | VB (μm) | SEM micrographs | KT (μm) | KM (μm) | VB (μm) | SEM micrographs | Workpiece roughness (μm) | Tool life (min) |
| Commercial | 3.69 | 325 | 108 | Fig. 2 | 7.64 | 157 | 50 | Fig. 4 | 12 | 42 |
| P3 | 3.6 | 187 | 667 | – | 2.10 | 192 | 47 | Fig. 5 | 4 | 33 |
| P7 | – | 139 | 22 | – | Fracture of the cutting edge | | | – | – | 6 |
| P10 | – | 181 | 69 | – | Fracture of the cutting edge | | | – | – | 12 |
| P6 | 3.07 | 176 | 35 | – | 3.32 | 200 | 34 | Fig. 3 | 11 | 25 |

KT—maximum crater depth; KM—distance between tool edge and crater centre; VB—maximum flank wear.

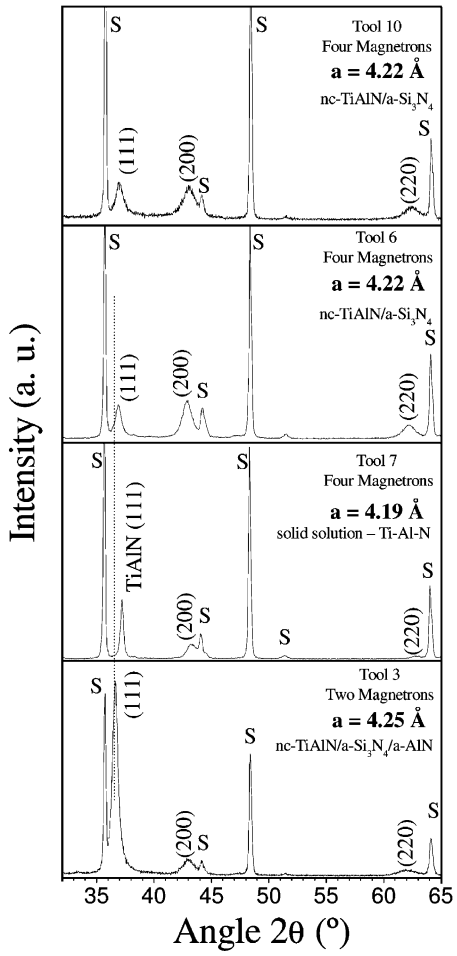


Fig. 1. XRD patterns of (Ti,Si,Al)N and (Ti,Al)N films deposited on tungsten carbide substrates.

tions are performed with simultaneous sputtering of both Ti(Si) and TiAl targets an increase in the lattice parameter is observed (tool 6 and 10). The lower Al content in these films (Table 1) can justify the shift of the diffraction peaks for lower angles in comparison with TiAlN film. For the sample produced with two magnetrons configuration (tool P3) a lattice parameter of 4.25 Å was derived. This must be related with an eventual segregation of Si atoms enhancing the formation of TiN and Ti(Al)N grains. In fact, if Si atoms were in substitution of Ti atoms in the TiN lattice, a decrease in the lattice parameter should be observed in relation to P6 and P10 films, which have lower Si content, due to the lower atomic radius of Si in comparison to Ti. The segregated Si atoms can be enough to nucleate and develop an amorphous matrix of $Si_3N_4$ [13,14,19]. Thus, the formation of a nc-TiN/a-$Si_3N_4$/nc-TiAlN should be expected. An Al segregation, with subsequent AlN precipitation, as already reported on (Ti,Al)N films [20], should not be considered taking into account the low lattice parameter found for this coating, indicating the presence of Al in solid solution in the cubic TiN lattice.

The shift observed in the peak position of P3 coated tool can also be attributed to the effect of the higher compressive residual stress measured in this coating (Table 1) in comparison to the other studied samples. Moreover, it presents a strong (1 1 1) preferential orientation whereas the other Si-containing films show the (2 0 0) and (2 2 0) crystallite growth. By increasing the ion bombardment the surface texture corresponding to the most open crystal channelling direction is favoured; for TiN the [1 1 1] direction exhibits the densest array of atom columns, while the [0 0 1] direction is the most open to channelling [21]. Both the presence of the compressive stress and the (1 1 1) preferential orientation can justify the higher hardness value measured in coated P3 tool in comparison to all the other coated inserts.

### 3.2. Cutting performance

#### 3.2.1. Wear evaluation: flank and rake wear

The cutting performance during the turning wear against an alloy steel of the coated tools was evaluated considering the maximum flank (VB) and rake wear (KM and KT) (Table 2).

For low cutting speeds (100 m/min), it was noticed that the commercial, P3 and P6 tools, reached a similar crater wear depth (KT)—evaluated by confocal microscope—after the same machining time. However, the flank wear is much higher for the commercial and P3 coated tools, particularly for this last insert. The difference in the performance of the tools should be related with the chip behaviour. In the beginning of the tests, the chips from the machining process were in the form of small fragments whatever was the coated insert, except for the P3 tool. During the last minutes of the cutting tests with the commercial and, particularly, with P3 tools the chip wound around the tool which can explain the greater maximum flank wear in these samples. The P3 tool showed a premature failure due to the very high value of the flank wear. The excessive flank wear modifies the insert geometry, deteriorating and weakening the cutting edge, causing premature tool failure. In these cases, temperatures up to 800 °C are easily attained in turning tests and so the tool is subjected to extreme mechanical and chemical loading [2]. Thermal load on the tool is mostly due the heat generation by the deformation work of the chip. Tools are protected from high thermal load as most of the heat is dissipated via chip removal. If the chips were not fractured during the turning test, as it is the case of those performed with the P3 tool at 100 m/min, the rolling of the chip around the tool or around the workpiece is observed, avoiding the liberation of the

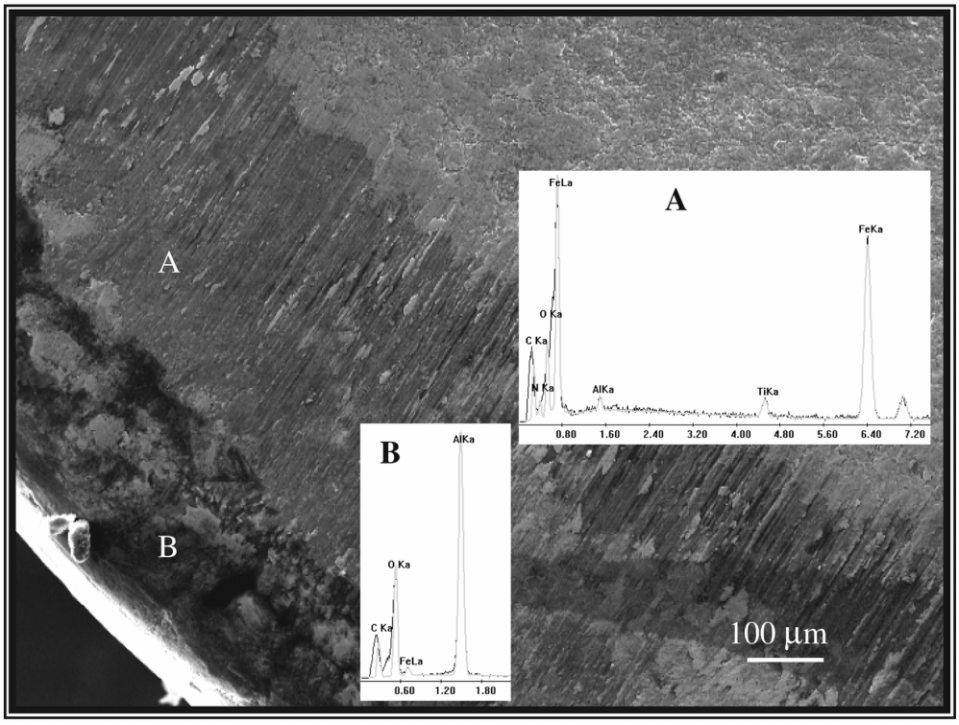


Fig. 2. SEM image of the commercial tool after turning test with $V_c = 100$ m/min, EDX spectra taken at points A and B.

thermal energy and contributing for the heating of the tool tip. The extreme heating of the cutting edge may enhance thermal cracks and consequently can originate premature failures in the tool surface. This increase in temperature, which was noticeable by observing that the cutting tool was incandescent and the chips turned blue due to the oxidation, must have induced the stress and structural relaxations in the (Ti,Si,Al)N coating of tool P3, leading to the decrease of both its mechanical strength and wear resistance.

For high cutting speeds two points can be remarked: first, the flank (VB) and rake (KM) wear values of the commercial, P3 and P6 are comparable, after 15 min of turning test. However, the depth of rake wear (KT) is significantly higher for the commercial tool although the high measured value ($\approx$7.6 μm) did not reach the total thickness of the coating ($\approx$15 μm). It seems that for similar turning conditions the cutting performance of P3 and P6 coated tools is better than that presented by the commercial insert. Secondly, the tools coated with (Ti,Si,Al)N showed a better cutting performance than the tool coated with the (Ti,Al)N. Indeed, a fracture of the cutting edge occurred for the (Ti,Al)N coated tool after 6 min, while P3 and P6 tools presented yet a cutting edge with acceptable conditions after 15 min, according to the ISO 3685 rules [22]. Finally, regarding the final surface finish of the steel workpiece, the (Ti,Si,Al)N coated tool outperformed the commercial tool, since the roughness of the workpiece in the former case is smaller (4 μm) than in the latter one (12 μm).

### *3.2.2. Wear mechanisms*

The micrographs in Figs. 2–5 illustrate the changes in rake and flank wear patterns of the tools after turning at several cutting conditions. In all the worn zones of the tested tools, iron contamination coming from the workpiece was detected (EDS (A) in all figures). The adherence of the workpiece material can be attributed to both the high plasticity of the austenitic fcc structure that work hardens rapidly and its reactivity with the tool material [23,24]. Oxidation of the test tool materials and debris of oxidized elements (Fe–O) coming from the workpiece were also possible to be detected by EDS. These results suggest that high temperatures are probably reached during the machining process, inducing the oxidation and softening phenomenas above described.

In the (Ti,Al)N tool chipping and coating delamination was observed by SEM. The EDS analysis on the worn surface of the tool P7 showed a high concentration of tungsten (W) and carbon (C) confirming the complete removal of the coating. On the other hand, an analysis of the wear crater of tool P6 revealed that, besides the zones with stick iron, many other places showed the presence of elements of the protective coating. Only in very small parts, limited coating delamination was detected. The delamination observed

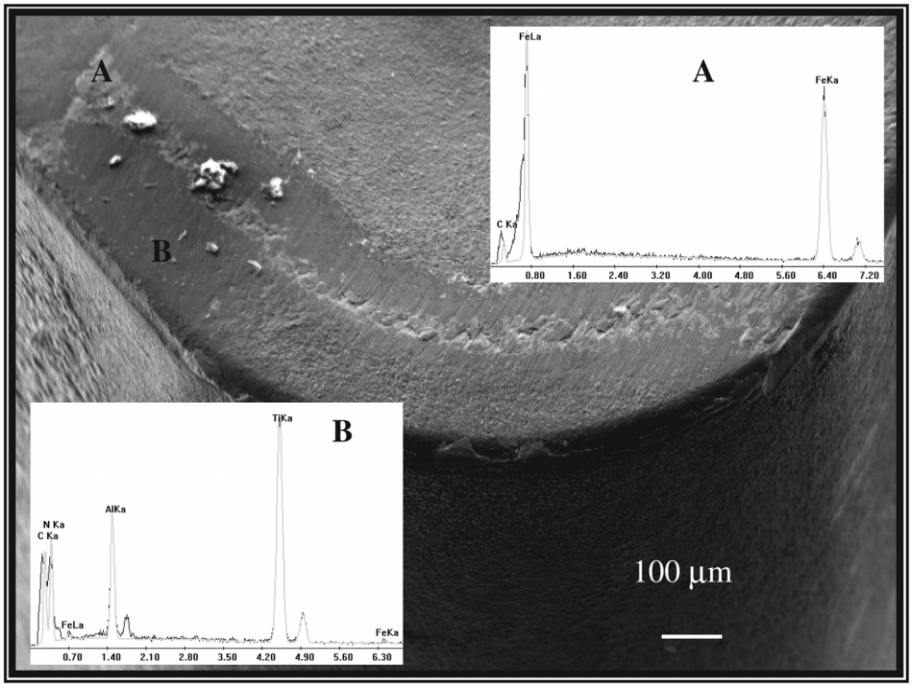


Fig. 3. SEM image of tool P6 after cutting 15 min at $V_c = 200$ m/min, showing the rake and flank face wear. The EDS (A) analysis on the worn region indicates adhesion or welding of the work material onto the rake face of the tool. EDS (B) analysis indicates that the (Ti,Si,Al)N coating has not yet been removed.

on PVD coatings could be attributed to crack propagation at the substrate interface and/or difference in the thermal coefficient of expansion between the coating matrix and the substrate and/or lower adhesion to the substrate comparing with CVD coatings [25].

A simple analysis of the values presented in Table 2, as example for the Tool 6 and 7 at 200 m/min, indicates that the Si content is determinant on the wear behaviour. With this cutting speed, the cutting edge of the (TiAl)N coated sample fractured after only 6 min of the turning

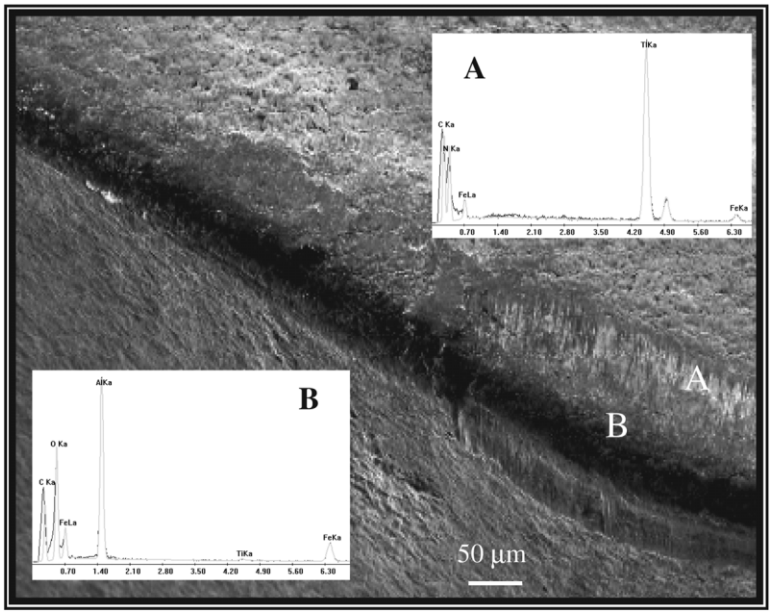


Fig. 4. Crater and flank wear of the commercial tool after machining 15 min at $V_c = 200$ m/min. EDS (A) analysis indicates that the TiN as well as $Al_2O_3$ coatings were removed.

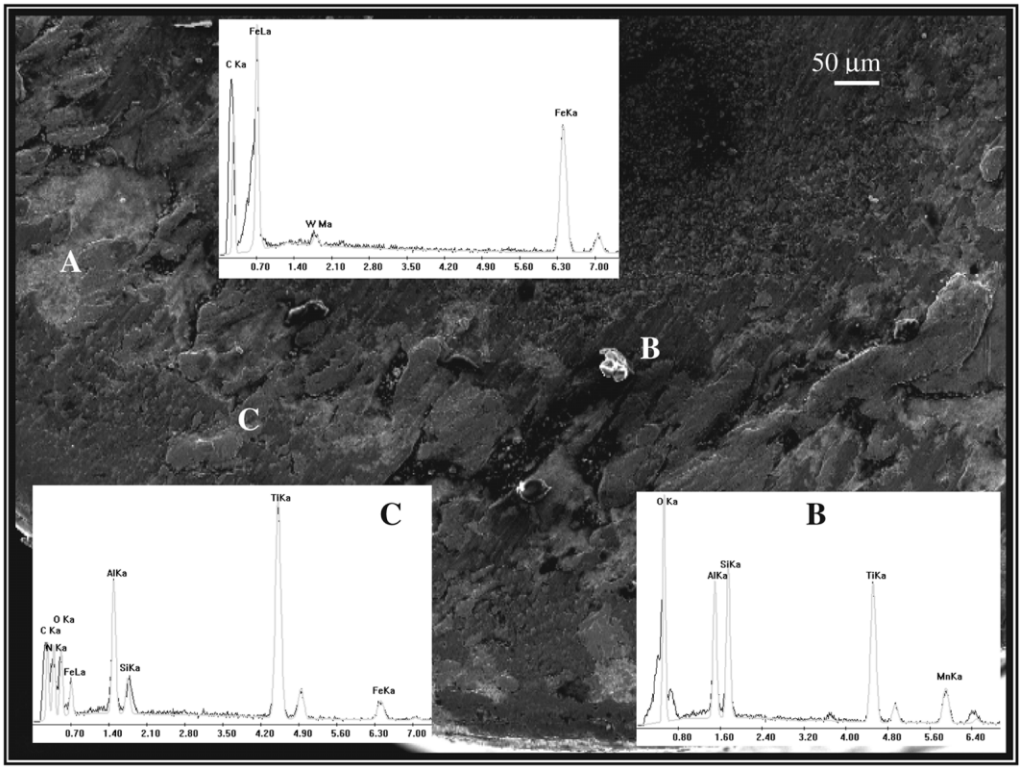


Fig. 5. Crater wear of the $Ti_{0.82}Si_{0.08}Al_{0.14}N_{0.96}$ (tool P3) after machining 15 min at $V_c = 200$ m/min. EDS (B) analysis denounces the formation of an oxide layer ($Al_2O_3$–$SiO_2$). EDS (C) analysis indicates that the (Ti,Si,Al)N coating has not been yet removed.

test, whereas P6 tool lasted for 15 min showing a very high resistance (Fig. 3). Adding Si to the (Ti,Al)N matrix changes the coating microstructure and structure, enhancing both the microhardness and oxidation resistance. Consequently, a superior wear behaviour of the (Ti,Si,Al)N films was achieved. Moreover, a promising wear performance of the (Ti,Si,Al)N coatings is also observed when comparing it to the wear pattern of the commercial tool (Figs. 4 and 5). Fig. 4 suggests that the CVD coating was strongly removed from the contact zone over the rake face of the tool. The EDS analysis taken on the worn areas indicates effectively that the top TiN layer has been completely removed as well as part of the intermediate $Al_2O_3$ coating, only the base Ti(C,N) layer remaining visible. On the contrary, Fig. 5 (tool P3) clearly shows that in spite of the galling consisting of a few thin layers of smeared workpiece material, (Ti,Si,Al)N coating has not yet been removed as demonstrated by the EDS (C) analysis.

## 4. Discussion

Richter and Ruthendorf [26] have previously shown that when a coating is exposed to oxidizing environments at elevated temperatures, oxidation of non-oxide compounds occurs. In the case of the samples studied in this work, EDS results showed that in many zones of the worn coated samples oxygen is clearly detected. For example in the case of tool P3, after the turning test, the (Ti,Si,Al)N coating developed an oxide layer composed by Ti, Si, Al and O, with a very small fraction of N (Fig. 5—EDS (B)). The atomic composition is different from that measured in the as-deposited sample (EDS (C)). When both compositions are compared, it seems that an Al + Si enrichment at the tool surface is observed after the turning test. The enrichment in Al + Si suggests the formation of an oxide layer of $Al_2O_3$–$SiO_2$, which should lead to a better oxidation resistance. For example, on (Ti,Al)N system, Vaz et al. [27] reported that films growing with a (1 1 1) texture developed at the high temperatures an oxide layered $Al_2O_3$–$TiO_2$ structure, which protects the underlying nitride from further oxidation.

Due to the high adhesive forces in dry machining processes, increased shear loads are induced in subsurface layers of the substrate and in the coating, as well as in the workpiece material. The shear loads induce the plastic deformation of the steel material and its adherence to the rank face of the cutting tool as

confirmed by the EDS results presented in Figs. 2–5. To avoid chipping in the cutting edge a high strength of the interface as well as of the coating itself is required [28]. The strength of a coated sample is often correlated with the Young's modulus, the hardness and the residual stress. The introduction of Si in the (Ti,Al)N-based matrix contributes for the strength improvement of (Ti,Al)N system and thus to its better in-service tribological behaviour.

The hardness enhancement in P3 and P6 coatings can also be apparently justified by the formation of a multilayer stacking of (Ti,Si)N/(Ti,Al)N, as was observed by HRTEM analysis [15]. The reason for the hardening effect in multilayers is that the introduction of multiple interfaces helps dissipating the crack tip energy and therefore strengthens the coating [29]. In the literature, large improvements in wear properties were reported for multilayered TiN/(Ti,Al)N coatings, as compared with the single-layer coatings [30]. An increase in the deposition rate induces the multilayer system formation and the corresponding increase in substrate temperature seems to be enough to ensure Si segregation with nc-TiN/a-$Si_3N_4$ formation from the (Ti,Si)N phase [15].

Further improvements concerning wear resistance of (Ti,Si,Al)N films can be expected by the following:

1. Increasing Si content, since P3 tool shows a superior cutting performance, probably due to its higher hardness. Indeed, a threshold Si content can ensure the optimum nanocrystal/amorphous phase segregation enhancing the hardening benefits attributed to this structural arrangement, as described by Veprek [8].
2. Thermal annealing before the turning tests in order to relax internal stresses, since recent tests revealed that after thermal annealing the tool life increased three times.

## 5. Conclusions

Within the frame of this work (Ti,Si,Al)N nanocomposites coatings were sputtered by PVD on tungsten carbide tools. The performance of these inserts was compared to a commercial tool and to (Ti,Al)N coated tool. In fact, the wear measured on the (Ti,Si,Al)N inserts, after turning an alloy steel during 15 min at a $V_c = 200$ m/min, is lower than that of the other inserts. This good wear behaviour should be related with

i. the addition of Si content that should induce an amorphous phase formation, consequently,
ii. the development of a multilayer (Ti,Si)N/(Ti,Al)N system that should strengthen the coating,
iii. the development of an oxide layer $Al_2O_3$–$SiO_2$ that should lead to a better oxidation resistance.

## Acknowledgments

The authors gratefully acknowledge the financial support of the 'Fundação para a Ciência e Tecnologia' (FCT) institution by the project no. POCTI/32670/CTM/2000 co-financed by European community fund FEDER and the financial support from the French–Portuguese agreement regarding the France Embassy/ICCTI institutions (program no. 543 B3/2001) and from the FCT/MCT pluri-annual program.

## References

[1] S.T. Buljan, S.F. Wayne, Wear 133 (1989) 309.
[2] R.F. Silva, J.M. Gomes, A.S. Miranda, J.M. Vieira, Wear 148 (1991) 69.
[3] M. Wittmer, J. Nose, H. Melchior, J. Appl. Phys. 52 (1981) 6659.
[4] P. Holubar, M. Jilek, M. Sima, Surf. Coat. Technol. 120–121 (1999) 184.
[5] T. Yoshida, Diam. Relat. Mater. 5 (1996) 501.
[6] D. McIntyre, J.E. Greene, G. Hakansson, J.E. Sundgren, W.D. Munz, J. Appl. Phys. 67 (1990) 1542.
[7] S. Hofmann, H.A. Jehn, Surf. Interf. Anal. 12 (1988) 329.
[8] S. Veprek, Surf. Coat. Technol. 97 (1997) 15.
[9] C. Mitterer, P.H. Mayrhofer, M. Beschliesser, P. Losbichler, P. Warbichler, F. Hofer, et al., Paper BP—16 presented at ICMCTF'99, Surf. Coat. Technol. 120–121 (1999) 405.
[10] X. Sun, J.S. Reid, E. Kolawa, M.-A. Nicolet, J. Appl. Phys 81 (2) (1997) 656.
[11] F. Vaz, Preparação e Caracterização de Revestimentos Duros Nanoestruturados de $Ti_{1-x}Si_xN_y$, preparados por Pulverização Catódica Reactiva em Magnetrão, Tese de Doutoramento, Univeridade do Minho, 2000.
[12] A. Niederhofer, P. Nesládek, H.-D. Männling, K. Moto, S. Veprek, M. Jílek, Surf. Coat. Technol. 120–121 (1999) 173.
[13] S. Carvalho, F. Vaz, L. Rebouta, D. Schneider, A. Cavaleiro, E. Alves, Surf. Coat. Technol. 142–144 (2001) 110.
[14] E. Ribeiro, A. Malczyk, S. Carvalho, et al., Surf. Coat. Technol. 152 (2002) 515.
[15] S. Carvalho, E. Ribeiro, L. Rebouta, et al., Surf. Coat. Technol. 172 (2002) 109.
[16] S. Carvalho, L. Rebouta, A. Cavaleiro, L.A. Rocha, J. Gomes, E. Alves, Thin Solid Films 398–399 (2001) 391–396.
[17] F. Vaz, L. Rebouta, M.F. da Silva, J.C. Soares, in: Y. Pauleau, P.B. Barna (Eds.), Protective Coatings and Thin Films, 1997, p. 501.
[18] O. Knotek, M. Böhmer, T. Leyendecker, J. Vac. Sci. Technol. A 4 (6) (1986) 2695.
[19] F. Vaz, L. Rebouta, B. Almeida, et al., Surf. Coat. Technol. 120–121 (1999) 166.
[20] J. Musil, H. Hrubý, Thin Solid Films 365 (2000) 104.
[21] I. Petrov, F. Adibi, J.E. Greene, L. Hultman, J.E. Sundgren, Appl. Phys. Lett. 63 (1993) 36.
[22] J. Paulo Davim, in: Almedina (Ed.), Princípios de Maquinagem, Coimbra, 1995, p. 126.
[23] A. Jawaid, S. Koksal, S. Sharif, J. Mater. Process. Technol. 116 (2001) 2.
[24] E.O. Ezugwu, I.R. Pashby, J. Mater. Process. Technol. 33 (1992) 429.
[25] D.Y. Wang, C.L. Chang, K.W. Wong, Y.W. Li, W.Y. Ho, Surf. Coat. Technol. 120–121 (1999) 388.

[26] V.A. Richter, M. Ruthendorf, Composition, microstructure, properties and cutting performance of cermets, EURO PM99, 1999, p. 229.
[27] F. Vaz, L. Rebouta, M. Andritscky, M.F. da Silva, J.C. Soares, Surf. Coat. Technol. 98 (1998) 912.
[28] K. Tönshoff, B. Karpuschewski, A. Mohlfeld, et al., Surf. Coat. Technol. 108–109 (1998) 535.
[29] J.S. Koehler, Phys. Rev. B 2 (1970) 547.
[30] S. PalDey, S.C. Deevi, Mat. Sci. Eng., in press.